ELSEVIER

Journal of Nuclear Materials 297 (2001) 129–137

journal of nuclear materials

www.elsevier.com/locate/jnucmat

Preliminary results on the leaching process of phosphate ceramics, potential hosts for actinide immobilization

L. Bois [a,*], M.J. Guittet [b], F. Carrot [a], P. Trocellier [a], M. Gautier-Soyer [b]

[a] *Laboratoire Pierre Süe, CEA, Saclay, F-91191 Gif/Yvette, France*
[b] *SRSIM, CEA, Saclay, F-91191 Gif/Yvette, France*

Received 11 January 2001; accepted 9 May 2001

Abstract

A mixed zirconium–lanthanum phosphate $La_{1/3}Zr_2(PO_4)_3$, noted LaZrP, is studied as a potential host for actinides issued from high-level nuclear wastes. Chemical durability is evaluated and compared with two other phases: a monazite phase $LaPO_4$, noted LaP, and a mixed oxide phase $La_{0.1}ZrO_{2.15}$, noted LaZrO. Leaching tests are performed and followed by solution and solid analyses. Static tests are performed with a low ratio between surface of ceramic and volume of solution, S/V (about 0.1 cm^{-1}). For LaZrP, the phosphate release rate decreases from 10^{-2} to 10^{-3} $g/m^2/day$, while zirconium and lanthanum releases remain very low ($<10^{-5}$ $g/m^2/day$). For the LaP phase, the phosphate release is about 10 times lower than for LaZrP and remains stationary, while the rate of the lanthanum release is below 10^{-6} $g/m^2/day$. Tests performed at high S/V (about 20 cm^{-1}) reveal that the lanthanum release rates after 2 weeks were, respectively, at 10^{-9}, 10^{-6} and 10^{-4} $g/m^2/day$ for LaP, LaZrP and LaZrO phases. It is shown that NZP or monazite type ceramics are highly resistant to the leaching process.

PACS: 28.41.T; 79.60; 81.05 J,M

1. Introduction

For the long-term storage of high-level nuclear wastes, development of chemically stable solid materials is required, more particularly for minor actinides specific storage.

Titanate-based ceramics, such as hollandite $BaAl_2Ti_6O_{16}$, perovskite $CaTiO_3$ and zirconolite or pyrochlore $CaZr_2Ti_2O_7$, have been the most widely studied ceramics waste forms [1–8]. Zirconolite, $CaZrTi_2O_7$, is the phase that tends to host the actinide elements [6,7]. Trivalent elements substitute in the Ca site of zirconolite while tetravalent substitute in the Zr site. Zircon, $ZrSiO_4$ was also proposed by Ewing et al. for the immobilization of U and Pu [9].

Synthetic phosphate mineral, which has a similar composition to monazite, (Ce, Y, La, Th)PO_4, has been developed as a high-level nuclear waste host [10–14]. Its corrosion behavior was investigated by Sales et al. [15,16] and the dissolution rate of the matrix was found to be at least 1000 times lower compared with a borosilicate glass.

Apatite $Ca_5(PO_4)_3$ (F, Cl, OH) has also been considered from natural analogous study, as well as phospho-silicate apatite, the britholite ceramic [17–21]. An important work on thorium and uranium phosphate has also been done and the thorium phosphate–diphosphate $Th_4(PO_4)_4P_2O_7$ has been proposed as a specific matrix for the storage of Pu and Np [22–25].

Zirconium hydrogeno-phosphate, widely studied as a mineral exchanger [26] has been proposed for the decontamination of radioactive solutions with ^{137}Cs and ^{90}Sr [27]. Another phosphate ceramic, the sodium zirconium phosphate $NaZr_2(PO_4)_3$ (NZP) was one of the candidate crystalline waste forms for the geological immobilization of high-level nuclear wastes [28–31]. Such

* Corresponding author. Present address: Service Central d'Analyse, Echangeur de Solaize, BP22, F-69390 Vernaison, France. Tel.: +33-4 78 02 22 84; fax: +33-4 78 02 71 87.
E-mail address: lbois@sca.cnrs.fr (L. Bois).

0022-3115/01/$ - see front matter
PII: S0022-3115(01)00607-9

phases, firstly proposed by Roy et al. [32–38], have numerous advantages: a high stability of the 3D network structure towards chemical substitution, a high waste loading, a refractory nature and an easy method of synthesis [39]. Moreover, they are resistant to radiation damage and dissolution.

The NZP structure results of a three-dimensional network of $(Zr_2P_3O_{12})^-$ units made up of corner-sharing ZrO_6 octahedra and PO_4 tetrahedra. The octahedral site is normally occupied by Zr^{4+}. The tetrahedral site is occupied by P^{5+} and two interstitial sites may or may not be occupied by Na^+. The site I has a distorted octahedral coordination and the site II has a trigonal prismatic coordination [40]. Divalent ions substitute for two alkali ions and rare-earth elements are assumed to occupy the Zr site.

Recently, members of the NZP structural family have been proposed as host materials for the actinides [28,29]. But the ability of the NZP framework to accommodate actinides has not been rigorously examined yet. Concerning the tetravalent actinides, the ability of $KZr_2(PO_4)_3$ to accommodate U(IV) has been evidenced for compounds in the series $KZr_{2-x}U_x(PO_4)_3$, $0 \leqslant x \leqslant 0.2$ [29]. The end member of the series $KA_2^{IV}(PO_4)_3$ A = U, Th, Np is known, with a monoclinic structure with a 9-fold coordination of A.

The present work reports on the synthesis of $La_{1/3}Zr_2(PO_4)_3$ (noted LaZrP), isostructural with the NZP phase and on the study of the leaching process of this compound. Lanthanum is used to simulate a trivalent minor actinide (Am, Cm). A lanthanum phosphate phase (monazite, noted LaP) is also studied, as well as a mixed lanthanum–zirconium oxide, noted LaZrO.

2. Experimental

2.1. Synthesis

2.1.1. LaZrP synthesis

Reaction precursors for the LaZrP synthesis, are zirconyl chloride octahydrate ($ZrOCl_2$, $8H_2O$), lanthanum nitrate hexa-hydrate $La(NO_3)_3$, xH_2O, phosphoric acid (H_3PO_4) and distilled water. Solutions of lanthanum and zirconium salts, prepared with reduced volume of deionized water are mixed together under conditions of constant stirring at room temperature. Phosphoric acid solution (50% in water) is then added dropwise and a paste is formed. The use of phosphoric acid may explain the pH decrease observed during the leaching experiment.

2.1.2. LaP synthesis

For the LaP preparation, lanthanum nitrate is dissolved in iso-propanol and a solution of phosphoric acid (10% in iso-propanol) is added to this solution, forming a paste.

2.1.3. LaZrO synthesis

For the LaZrO preparation, lanthanum nitrate is dissolved in iso-propanol and zirconyl isopropoxide (70% in iso-propanol) is added to this solution. Then a mixture of water ($H_2O/Zr = 2$) and isopropanol (10% of water) is added, forming a paste.

Pastes are dried at 25°C a few days. Resulting materials are ground in an agate mortar and calcined at 600°C at a rate of 2°C/min, during 15 h. Pellets were obtained by pressing (at 5 MPa) and then sintering at 1000°C at a rate of 2°C/min, during 24 h. The pellet density was measured and the microstructure was examined by SEM. The grain size distribution was not available.

Powders obtained by grinding the sintered samples are characterized with an X-ray diffractometer which utilized CuKα radiation. Data are collected from 10° to 50° 2θ with a 0.05° 2θ step at 2 s/step.

The infrared spectra are recorded in the range 2000–400 cm^{-1} using the KBr disk technique or with a specular reflectance device.

2.2. Leaching experiments

The leaching experiments are performed in a Teflon recipient (savillex). Each leaching test was triplicated. Experiments were performed using ceramic surface area (S) (assumed equal to geometrical surface) to solution volume (V) ratios of 0.1 cm^{-1} (using monoliths), and 18 cm^{-1} (using powders; calculated value). It should be noted that this value is just an estimation and that a BET measurement could give a very different result. Leaching time varied from a few days to six months for a low S/V experiment and was of 15 days for a high S/V experiment. The temperature is chosen to be 96°C (in order to avoid boiling and to accelerate the kinetic). In the case of tests with powders, a quantity of 2 g (75–150 μm) is used with a volume of leachant (deionized water) 20 ml, respectively. In the case of tests using pellets, a pellet of 500 mg (diameter 13 mm) is used with a volume of leachant of 25 ml. No washing procedure was used as it should have been.

2.3. Analyses of leachates

After cooling, the pH of the leachate is measured with a combined glass electrode. The leachate is filtered (0.45 μm), acidified with Normatom nitric acid (65%) to pH about 2, and kept in a polypropylen vial. The solution is analyzed in order to detect La and Zr by ICP–MS. Each analysis is repeated three times and the relative error of the measurement is about 1–2%. The relative error introduced by diluting the leachate is

below 10%. Spectrophotometry analysis is used to determine phosphate concentration in the leachate, according to the molybdenum vanadate complex method (*Merck spectroquant*). Relative errors on aqueous concentration are estimated to less than 10%.

2.4. Analysis of altered surface using X-ray photoelectron spectroscopy (XPS)

The exciting X-ray source is a non-monochromatic AlK_α (1486.6 eV). Pressure in the sample chamber is kept at less than 2×10^{-10} mbar. Surface and thickness analyzed are about 1 $cm^2 \times 20$ Å. The Zr_{3d}, $La_{3d5/2}$, P_{2p} and O_{1s} concentrations (at.%) are derived from the Zr_{3d}, $La_{3d5/2}$, P_{2p} and O_{1s} photoelectron line intensities corrected by the ionization cross-sections.

3. Results and discussion

3.1. Characterization of unleached phases

Theoretical density of LaZrP is of 3.33 [41]. An experimental density of 3.13 (94% of the theoretical density) has been measured. Theoretical density of LaP is of 5.26 [16]. The density of LaP was measured at 4.70 (89% of the theoretical density).The microstructures are shown in Fig. 1, where it can be noted that the densification is not completed.

X-ray diffraction analysis of the ceramic LaZrP, reveals the formation of a phase isostructural with the $Eu_{1/3}Zr_2(PO_4)_3$, phase synthesized by Talbi et al. [41], and with the well-known $NaZr_2(PO_4)_3$ (NZP) phase [42] (Fig. 2(a)).

Two minor phases ZrP_2O_7 and α-$Zr_2O(PO_4)_2$ are also present [42]. The slow decomposition after 900°C of the $Zr_{0.25}Zr_2(PO_4)_3$ phase into ZrP_2O_7 and α-$Zr_2P_2O_9$ was already noted [43]. Below 1000°C, the decomposition occurs, according to the reaction [41]:

$$Ln_{1/3}Zr_2(PO_4)_3 \rightarrow 2/3ZrP_2O_7 + 2/3Zr_2P_2O_9 + 1/3LnPO_4.$$

Above 1000°C, zirconium diphosphate is decomposed as follows:

$$ZrP_2O_7 \rightarrow Zr_2P_2O_9 + P_2O_5.$$

The LaP phase has been identified as a monazite phase [42] (Fig. 2(b)). However, a minor phase is also observed, identified as lanthanum oxide La_2O_3 [42]. The roughly estimated level for this compound is about 10%.

The infrared spectrum of LaZrP (Fig. 3(a)), measured with the KBr-method, consists of vibration bands at 1160, 1110, 1063, 980, 950 and 935 cm^{-1}. Three other bands at 644, 555 and 435 cm^{-1} are also noted at lower frequencies. The first four vibration bands may be attributed to the anti-symmetric stretching of P–O bonds [24]. The vibration band at 935 cm^{-1} is probably due to the symmetric stretching of the P–O bond, while at lower frequencies, the bending vibrations of the P–O bond are observed. The phosphate ν_{as} vibrations in the LaP phase (Fig. 3(c)) are at lower frequencies compared with the ZrP phase (Fig. 3(b)), which is due to the higher molecular weight of lanthanum. The phosphate ν_{as} vibrations in LaZrP (Fig. 3(a)) cover the range observed in ZrP and LaP phases.

In order to observe the leaching process at the ceramic surface, experiments have been performed with a specular reflectance device (Figs. 4(a)–(b)). Compared

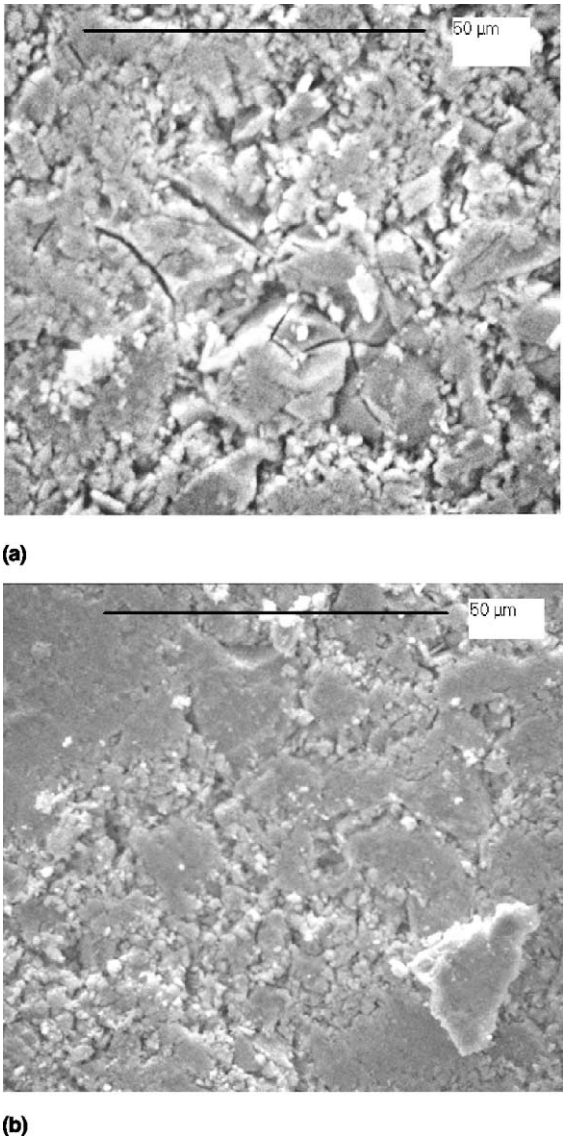

Fig. 1. SEM photographs of LaZrP (a) and LaP (b) ceramics.

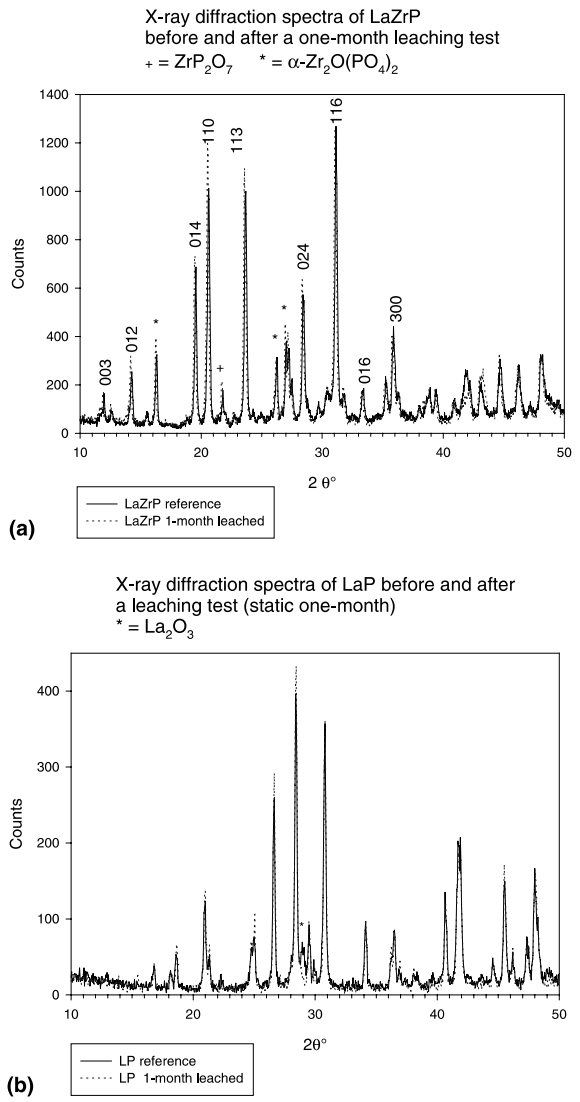

Fig. 2. X-ray diffraction spectra of: LaZrP (a) and LaP (b) ceramics.

with the transmission experiment, the vibrations bands are observed at about the same positions, but intensities are quite different, since bending vibrations are almost not observed (not represented).

X-ray photoelectron spectra are shown in Fig. 5. The $La_{3d5/2}$ core photoelectron line of LaZrP is located at 836.5 ± 0.1 eV (Table 1). The O_{1s} photoelectron line is located at 531.2 ± 0.1 eV. The P_{2s} photoelectron line is at 190.7 eV. The $Zr_{3d5/2}$ photoelectron line position is noted at 182.7 ± 0.1 eV. The P_{2p} photoelectron line is at 133.1 ± 0.1 eV. The $La_{4d5/2}$ is at 103.7 ± 0.1 eV.

The $La_{3d5/2}$ core photoelectron line of LaP is located at 835.9 eV, at 0.8 eV lower energy compared with the LaZrP phase (Table 1). The O_{1s} photoelectron line is located at 531.4 eV. The P_{2p} photoelectron line is at 133.4 eV. The $La_{4d5/2}$ is at 103.2 eV.

3.2. Leaching process

3.2.1. Leaching process at low S/V

3.2.1.1. LaZrP leaching process. Solution analyses of the leaching experiments at low S/V ratio of LaZrP are reported in Table 2. Neither zirconium release nor lanthanum release was noted. An important phosphor release was observed, even after two days, associated to a pH decrease from 5.5 to 4. The presence of $H_2PO_4^-$ and HPO_4^{2-} (acidity constants at 2.1 and 7.2) should explain the pH decrease. A preliminary washing step would probably have overcome this artifact.

3.2.1.2. LaP leaching process. In the case of the LaP ceramic, solution analyses for low S/V ratio experiments (Table 2) reveal a very low lanthanum release, associated to a phosphate release about, 10 times lower than in the case of the LaZrP ceramic, with a pH increase to 9. The dissolution of the lanthanum oxide phase may explain the pH increase.

$$La_2O_3 + 3H_2O \rightarrow 2La^{3+} + 6OH^-.$$

3.2.1.3. Phosphor release. The phosphor release versus time in LaZrP leaching experiment strongly increases within the first days and then increases more slowly, as shown in Fig. 6. It is stationary in the case of the LaP leaching test (Fig. 6). The intrinsic dissolution rate of these ceramics is probably well estimated by the phosphor release as phosphor is a structural former.

3.2.1.4. Rates of dissolution. Rates of dissolution (in $g/m^2/day$) have been calculated from solution analyses. For this calculation, elemental releases (ppm) have been normalized to the time, to the elemental weight percent and to the S/V ratio. In the case of low S/V experiment, the S/V ratio is assumed to be about 0.1 cm^{-1}, using the geometrical surface. In the case of high S/V experiment, an S/V ratio of 18 cm^{-1} is estimated, using an average diameter of the ceramic particles of 100 μm. These values are only estimations and a BET measurement could give a very different result.

The rate of phosphate release is about 10^{-2} $g/m^2/day$ the first days and then decreases to 3×10^{-3} $g/m^2/day$. The rate of lanthanum release is below 10^{-6} $g/m^2/day$.

3.2.2. Leaching process at high S/V

3.2.2.1. LaZrP leaching process. At high S/V, after two weeks (Table 3), releases in LaZrP are equivalent with those measured after a six-month experiment at low

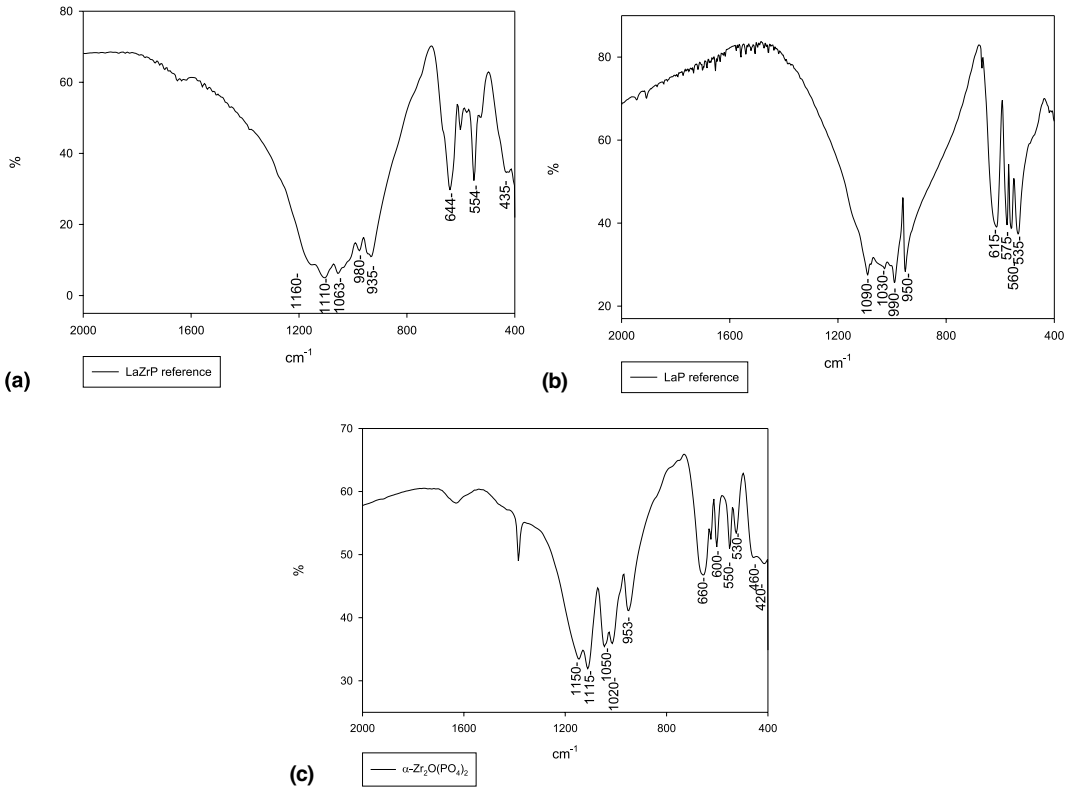

Fig. 3. Infrared spectra (transmission) of: LaZrP (a), LaP (b) and ZrP (c) ceramics.

S/V. Lanthanum and zirconium releases are very low: about 10 ppb, while phosphate release is about 5 ppm.

3.2.2.2. LaP leaching process. For experiments on LaP (Table 3), lanthanum and phosphate releases are similar with those obtained at low S/V ratio.

3.2.2.3. Rates of dissolution. A comparison of the leaching rates after a two-week experiment (Table 3) of the LaZrP, and LaP ceramics as well as a mixed oxide La_2O_3–ZrO_2, reveals that the retention of lanthanum in the LaP phase is very good (10^{-9} g/m^2/day), quite good in the LaZrP system (10^{-6} g/m^2/day) and very limited in the La_2O_3–ZrO_2 system (10^{-4}–10^{-3} g/m^2/day). In the LaZrP phase, lanthanum and zirconium are almost not released, while phosphor is about 100 times more released. The same difference is noted in the LaP phase. In the case of the LaZrO phase, lanthanum is not retained in the solid phase, while zirconium remains unsoluble.

One possible explanation for these differences is that in the presence of phosphate ions, secondary solid phosphate phases are precipitating with lanthanum. This could not be the case for La_2O_3–ZrO_2-based components, so the dissolved lanthanum amounts are larger.

Similar results were obtained by Zyrianov and Vance [30]: leaching rates of 10^{-8} g/m^2/day for Zr, 2×10^{-7} g/m^2/day for Nd and 2×10^{-3} g/m^2/day for P after a leaching experiment of 28 days at 90°C were measured on $Na_{0.5}Ca_{0.5}Nd_{0.5}Zr_{1.5}(PO_4)_3$. The lanthanum release rate in monazite was measured at 10^{-6} g/m^2/day [15], while the matrix dissolution rate is reported at 2×10^{-3} g/m^2/day [14]. The dissolution rate of thorium phosphate–diphosphate was measured at 10^{-7} g/m^2/day [25].

3.3. Analysis of altered surfaces

Evolution of the solid phases is also observed. Observation of the altered surface by SEM reveals no change; more specially, no secondary phases are noted. There is almost no modification of the XRD spectrum (acquired with a pellet) after a leaching experiment, except that the peak at 41.7° is no more observed in the case of LaZrP (Fig. 2(a)). The diffraction peak attributed to La_2O_3 in the LaP spectrum has disappeared (Fig. 2(b)). Leaching process induces a shift to lower frequencies of the infrared ν_{as} P–O vibration band at 1200 cm^{-1} (Fig. 4(a)). This shift to lower frequencies is also observed in the case of the LaP ceramic (Fig. 4(b)).

An analysis of the intensities of the main photoelectron lines of LaZrP (Table 4) reveals that there is a

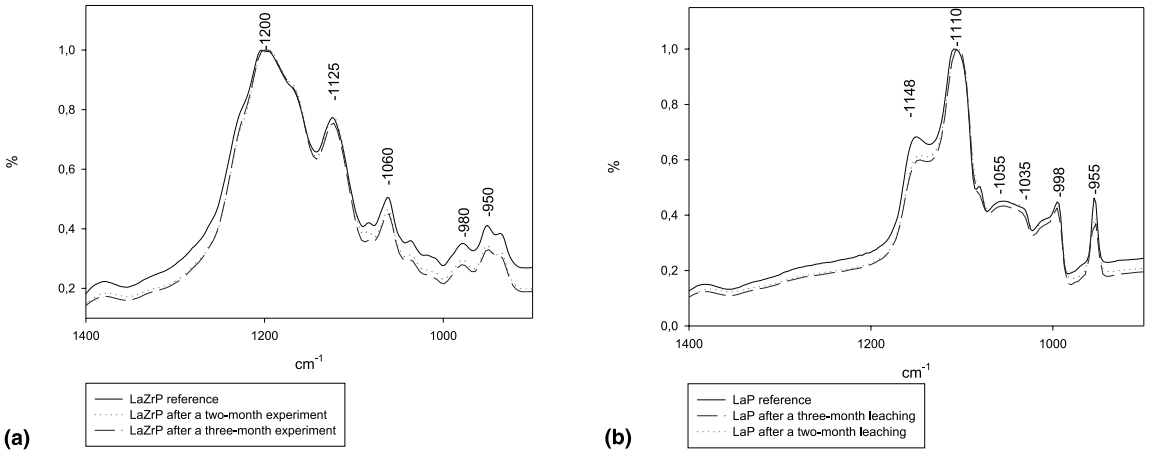

Fig. 4. Infrared spectra (reflexion) of: LaZrP (a) and LaP (b) ceramics before and after the alteration process.

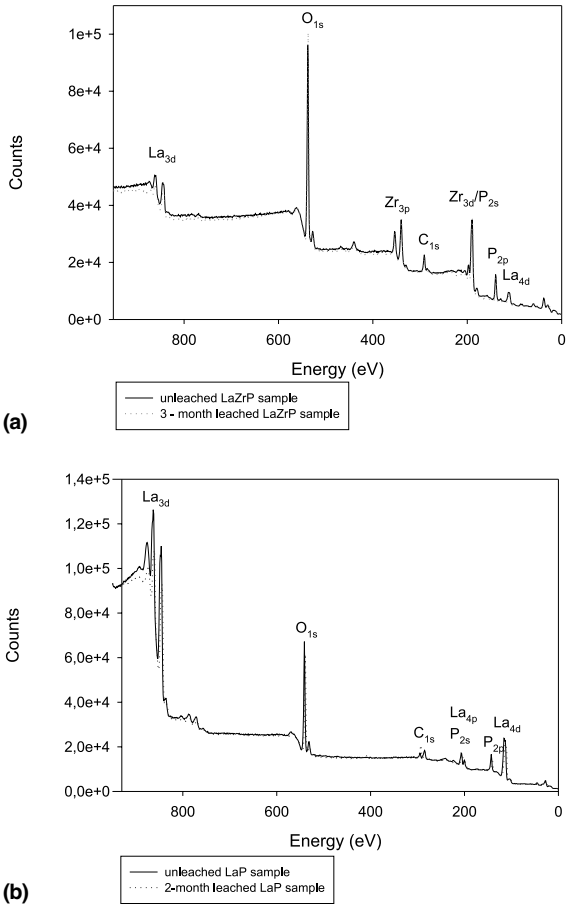

Fig. 5. X-ray photoelectron spectra of: LaZrP (a) and LaP (b) ceramics before and after the alteration process.

decrease of the $La_{3d5/2}$ from 2.5 ± 0.3 to 1.7 ± 0.1 after a three-month leaching test. The Zr_{3d} intensity is slightly increased from $11.9 \pm 0.5\%$ to $12.2 \pm 0.1\%$.

Then, the $Zr_{3d}/La_{3d5/2}$ ratio is clearly increased from 4.8 to 7.2 (Fig. 7). The same evolution is noted after a high S/V test, where the $Zr_{3d}/La_{3d5/2}$ ratio has increased from 4.8 to 9.2. No differences are noted concerning the P_{2p}/Zr_{3d} and O_{1s}/Zr_{3d} ratios. Almost no difference is noted on the energies of the main photoelectron lines. The analysis of the leaching process of the LaP ceramics reveals no change of the intensities and of the energies of the main photoelectron lines (Tables 1 and 5).

3.4. Discussion

The dissolution reaction of LaZrP is represented by the following equation:-

$$La_{1/3}Zr_2(PO_4)_3 + 8H_2O \rightarrow 1/3La^{3+} + 2Zr(OH)_4 + 3H_2PO_4^- + 2H^+.$$

If the dissolution was congruent, lanthanum, zirconium and phosphor should be found in the solution. But solution analyses have shown almost only a phosphor release. A preliminary washing step should be introduced to eliminate residual phosphoric acid. Moreover, precipitation reactions of zirconium hydroxides and lanthanum hydroxycarbonates may explain the non-congruency. But there are still some contradictions between solution and solid analyses, since solution analyses reveal a loss of phosphate, while surface analyses show a small loss of lanthanum.

The dissolution reaction of LaP is represented by the following equation:

$$LaPO_4 \rightarrow La^{3+} + PO_4^{3-}.$$

Concerning the LaP experiment, there is a good accordance between the very low solution releases and the absence of evolution of the ceramic surface, except the disappearance of the La_2O_3 phase should be associated to a lanthanum solution release, which means that

Table 1
Energies of the photoelectron lines before and after the alteration process in LaZrP and LaP ceramics

Energy (eV)	$La_{3d5/2}$	O_{1s}	P_{2s}	Zr_{3d}	P_{2p}	La_{4d}
LaZrP reference	836.5 ± 0.1	531.2 ± 0.1	190.7	182.7 ± 0.1	133.1 ± 0.1	103.7 ± 0.1
LaZrP low S/V 15-day	836.2 ± 0.1	531.0 ± 0.1	190.6	182.5 ± 0.1	133.0 ± 0.1	103.4
LaZrP low S/V 1-month	836.3 ± 0.1	531.1	190.6	182.5 ± 0.1	133.1	103.5 ± 0.1
LaZrP low S/V 2-month	836.2 ± 0.1	531.0 ± 0.1	190.6	182.6 ± 0.1	133.0 ± 0.1	103.5
LaZrP low S/V 3-month	836.4	531.2 ± 0.1	190.7	182.8 ± 0.1	133.3 ± 0.2	103.7 ± 0.1
LaZrP high S/V 15-day	836.4 ± 0.1	531.2 ± 0.1	190.7	182.8 ± 0.1	133.2	103.6
LaP reference	835.9	531.4			133.4	103.2
LaP low S/V 1-month	835.4 ± 0.3	530.9 ± 0.3			132.75 ± 0.3	102.7 ± 0.4
LaP low S/V 2-month	835.4 ± 0.1	530.80 ± 0.1			132.70 ± 0.1	102.7 ± 0.1
LaP high S/V 15-day	835.8	531.3			133.3	103.3
ZrP reference		531.4		182.9	133.6	

Table 2
Elemental releases and leaching rates ($g/m^2/day$) of LaZrP, LaP (leaching tests with low S/V)

Ceramic	Element	1-month	2-month	3-month	6-month
LaZrP	La ppb	0.2	0.2	0	0
	La $g/m^2/day$	7.3×10^{-6}	3.6×10^{-6}		
	Zr ppb	0.2	0.1	0	0
	Zr $g/m^2/day$	1.9×10^{-6}	4.7×10^{-7}		
	PO_4 ppm	2.6	2.1	3.2	4.8
	P $g/m^2/day$	2.3×10^{-3}	1.2×10^{-2}	8.1×10^{-3}	3.6×10^{-3}
	Final pH	4.0	4.1	4.1	3.8
LaP	La ppb	3.0	0.26	0.28	0.60
	La $g/m^2/day$	1.7×10^{-5}	7.3×10^{-7}	5.2×10^{-7}	5.6×10^{-7}
	PO_4 ppm	0.3	0.3	0.7	0.1
	P $g/m^2/day$	2.4×10^{-3}	1.2×10^{-3}	1.9×10^{-3}	1.4×10^{-4}
	Final pH	7.9	8.7	9.0	8.0

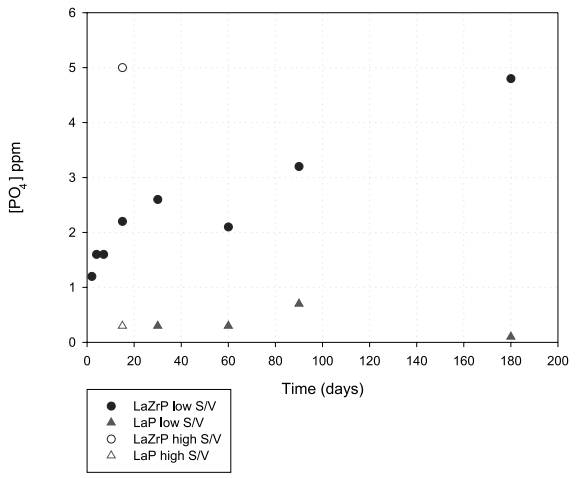

Fig. 6. Phosphate releases versus time during the alteration process of LaZrP and LaP ceramics.

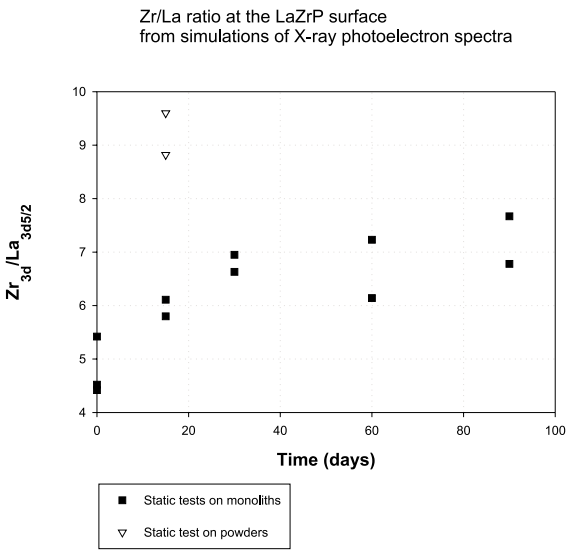

Fig. 7. $Zr_{3d}/La_{3d5/2}$ intensities ratio versus time (from X-ray photoelectron spectra) during the leaching of LaZrP ceramic.

Table 3
Elemental releases and leaching rates ($g/m^2/day$) for LaZrP, LaP and LaZrO (leaching tests with high S/V)

Element	Ceramic		
	LaZrP	LaP	LaZrO
La ppb	6.3	0.04	493.6
La $g/m^2/day$	2.5×10^{-6}	2.5×10^{-9}	1.6×10^{-4}
Zr ppb	13.5	–	0.6
Zr $g/m^2/day$	1.4×10^{-6}		5.1×10^{-7}
PO_4 ppm	5.0	0.3	–
P $g/m^2/day$	3.2×10^{-4}	2.7×10^{-5}	
Final pH	4.1	9.3	6.3

Table 4
Intensities (%) of the photoelectron lines before and after the alteration process in LaZrP ceramic

Percentage	$La_{3d5/2}$	O_{1s}	Zr_{3d}	P_{2p}	O_{1s}/Zr_{3d}	P_{2p}/Zr_{3d}	$Zr_{3d}/La_{3d5/2}$
LaZrP theoretical	1.9	69.2	11.5	17.3	6.0	1.5	6.0
LaZrP reference	2.5 ± 0.3	66.5 ± 1.5	11.9 ± 0.5	19.1 ± 1.0	5.6 ± 0.3	1.6 ± 0.1	4.8 ± 0.5
LaZrP low S/V 15-day	2.0 ± 0.1	65.6 ± 0.5	12.3 ± 0.3	19.9 ± 0.2	5.3 ± 0.2	1.6 ± 0.1	5.9 ± 0.2
LaZrP low S/V 1-month	1.9 ± 0.1	66.7 ± 0.1	12.8 ± 1.0	18.5 ± 1.0	5.2 ± 0.3	1.4 ± 0.2	6.8 ± 0.2
LaZrP low S/V 2-month	1.8 ± 0.2	66.6 ± 1.0	12.1 ± 0.2	19.3 ± 0.7	5.5 ± 0.1	1.6 ± 0.05	6.7 ± 0.6
LaZrP low S/V 3-month	1.7 ± 0.1	66.9 ± 0.5	12.2 ± 0.1	19.1 ± 0.5	5.4 ± 0.1	1.5 ± 0.1	7.2 ± 0.4
LaZrP high S/V 15-day	1.3 ± 0.1	67.1 ± 0.5	12.5 ± 0.4	18.9 ± 0.1	5.3 ± 0.3	1.5 ± 0.05	9.2 ± 0.4

Table 5
Intensities (%) of the photoelectron lines before and after the alteration process in LaP ceramic

Percentage	$La_{3d5/2}$	O_{1s}	P_{2p}	$O_{1s}/La_{3d5/2}$	$P_{2p}/La_{3d5/2}$
LaP theoretical	16.6	66.6	16.6	4.0	1.0
LaP reference	17.1 ± 0.1	60.0 ± 0.2	22.9 ± 0.4	3.5	1.3
LaP low S/V 1-month	15.2 ± 0.6	63.1 ± 0.8	21.6 ± 0.2	4.1	1.4
LaP low S/V 2-month	15.4 ± 0.2	64.4 ± 0.4	20.1 ± 0.6	4.1	1.3
LaP high S/V 15-day	16.6	63.2	20.1	3.8	1.2

precipitation reactions (of lanthanum hydroxycarbonates, carbonate or phosphate for instance) have also taken place.

The presence of phosphate in the ceramic prevents lanthanum from leaching and explains the excellent chemical durability of these phases. Lanthanum phosphate phases may be formed and control the lanthanum solubility to a very low level.

4. Conclusion

In order to get ceramic phases for specific storage of long-life actinide, ceramics $LaPO_4$ and $La_{1/3}Zr_2(PO_4)_3$ (NZP-type) are prepared by precipitation of salt solutions with phosphoric acid. Their leaching properties are then evaluated, lanthanum releases simulating actinide releases. It has been shown that NZP- or monazite-type ceramics are highly resistant to leaching process. In the low S/V experiments, lanthanum releases from LaZrP ceramics are almost below the detection limits ($<10^{-5}$ $g/m^2/day$). Phosphor release is however quite important between 10^{-2} and 10^{-3} $g/m^2/day$. The phosphor release gives the best estimate of the intrinsic dissolution rate of these ceramic as phosphor is a structural former. XPS analysis shows a decrease of the $La_{3d5/2}/Zr_{3d}$ ratio. Lanthanum releases from LaP ceramics are below 10^{-6} $g/m^2/day$, while phosphor release is stationary and 10 times lower compared with the LaZrP case. In the high S/V experiments, lanthanum releases increase from 10^{-9}, 10^{-6} and 10^{-4} $g/m^2/day$ between the LaP, LaZrP and LaZrO, respectively. At high S/V, secondary phosphate phases are probably formed and control the lanthanum release rate.

Acknowledgements

We would like to acknowledge N. Blanchard (LLB, CEA, Saclay) for her support during X-ray diffraction experiments.

References

[1] A. Navrotsky, Actinides and the Environment, Kluwer Academic, Dodrecht, 1998, p. 267.
[2] V.M. Oversby, in: R.W. Cahn, P. Haasen, E.J. Kramer (Eds.), Nuclear Materials, vol. 10B, 1994.
[3] I.W. Donald, B.L. Metcalfe, R.N.J. Taylor, J. Mater. Sci. 32 (1997) 5851.
[4] A.E. Ringwood, S.E. Kesson, K.D. Reeve, in: W. Lutze, R.C. Ewing (Eds.), Radioactive Waste Forms for the Future, 1988, p. 233.
[5] T. Advocat, G. Leturcq, Mater. Res. Soc. 465 (1997) 355.
[6] G. Leturcq, C.R. Acad, Science 327 (1998) 827.
[7] S.K. Roberts, Radiochim. Acta 88 (9–11) (2000) 539.
[8] K. Kuramoto, H. Mitamura, T. Banda, Prog. Nucl. Energy 32 (1998) 509.
[9] R.C. Ewing, W. Lutze, W.J. Weber, J. Mater. Res. 10 (1995) 243.
[10] F.J. Ryerson, J. Am. Ceram. Soc. 67 (1984) 75.
[11] A.E. Ringwood, S.E. Kesson, Nature 278 (1979) 219.
[12] R.J. Floran, M.M. Abraham, Sci. Basis Nucl. Waste Manage. 3 (1981) 507.
[13] M.M. Abraham, L.A. Boatner, Nucl. Waste Manage. 1 (1980) 181.
[14] G. McCarty, W.B. White, Mater. Res. Bull. 13 (1978) 1239.
[15] B.C. Sales, C.W. White, Nucl. Chem. Waste Manage. 4 (1983) 281.
[16] L.A. Boatner, B.C. Sales, in: W. Lutze, R.C. Ewing (Eds.), Radioactive Waste Forms for the Future, 1988, p. 495.
[17] S.V. Raman, J. Non-Cryst. Solids 263 (2000) 395.
[18] G. Buvaneswari, U.V. Varadaraju, J. Solid State Chem. 149 (2000) 133.
[19] L. Boyer, J.M. Savariault, Acta Crystallogr. 54 (1998) 1057.
[20] J. Carpéna, J.L. Lacout, L'Act. Chim. 2 (1997) 3.
[21] R. Gauglitz, M. Holterdorf, W. Franke, Radiochim. Acta 58&59 (1992) 253.
[22] P. Bénard, V. Brandel, Chem. Mater. 8 (1996) 181.
[23] N. Dacheux, R. Podor, J. Nucl. Mater. 252 (1998) 179.
[24] N. Dacheux, PhD, University Paris XI, 1995.
[25] E. Pichot, PhD, University Paris XI, 1999.
[26] A. Clearfield, Chem. Rev. 88 (1988) 125.
[27] M. Zamin, T. Shaheen, J. Radioanal. Nucl. Chem. 182 (1994) 335.
[28] H.T. Hawkins, B.E. Scheetz, G.D. Guthrie, Mater. Res. Soc. 465 (1997) 387.
[29] H.T. Hawkins, D.R. Spearing, Chem. Mater. 11 (1999) 2851.
[30] V.N. Zyrianov, E.R. Vance, Mater. Res. Soc. 465 (1997) 409.
[31] A.I. Orlova, V.N. Zyryanov, A.R. Kotel'nikov, Radiochemistry 35 (1993) 717.
[32] R. Roy, E.R. Vance, J. Alamo, J. Mater. Res. Bull. 17 (1982) 585.
[33] R. Roy, L.J. Yang, Mater. Res. Soc. 15 (1983) 15.
[34] B. Scheetz, D.K. Agrawal, E. Brewal, Waste Manage. 14 (1994) 489.
[35] B.E. Scheetz, R. Roy, in: W. Lutze, R.C. Ewing (Eds.), Radioactive Wastes Forms for the Future, 1988, p. 586.
[36] L.-J. Yang, S. Komarneni, R. Roy, Nucl. Waste Manage. 8 (1984) 377.
[37] B.E. Scheetz, S. Komarneni, W. Fajun, Mater. Res. Soc. 44 (1985) 903.
[38] E.R. Vance, F.J. Ahmad, Mater. Res. Soc. 15 (1983) 105.
[39] M. Sugantha, N.R.S. Kumar, Waste Manage. 18 (1998) 275.
[40] G. Buvaneswari, U.V. Varadaraju, J. Solid State Chem. 145 (1999) 227.
[41] M.A. Talbi, R. Brochu, C. Parent, J. Solid State Chem. 110 (1994) 350.
[42] NZP, JCPDS file number: 70-0233, ZrP_2O_7, JCPDS file number: 03-0261, α-$Zr_2O(PO_4)_2$ JCPDS file number 38-0018, $LaPO_4$ JCPDS file number 84-0600, La_2O_3 JCPDS file number 83-1355.
[43] J. Alamo, R. Roy, Commun. Am. Ceram. Soc. (1984) C80.